Since January 2020 Elsevier has created a COVID-19 resource centre with free information in English and Mandarin on the novel coronavirus COVID-19. The COVID-19 resource centre is hosted on Elsevier Connect, the company's public news and information website.

European Journal of Radiology 81 (2012) 389–394

Contents lists available at ScienceDirect

European Journal of Radiology

journal homepage: www.elsevier.com/locate/ejrad

Computed tomography findings from patients with ARDS due to Influenza A (H1N1) virus-associated pneumonia

Christian Grieser[a,*,1], Anton Goldmann[b,1], Ingo G. Steffen[a], Marc Kastrup[b], Carmen María Pérez Fernández[a], Ulrike Engert[a], Maria Deja[b], Christian Lojewski[b], Timm Denecke[a]

[a] Klinik für Strahlenheilkunde, Campus Virchow-Klinikum, Charité–Universitätsmedizin Berlin, Germany
[b] Klinik für Anästhesiologie, Campus Virchow-Klinikum, Charité–Universitätsmedizin Berlin, Germany

ARTICLE INFO

Article history:
Received 7 November 2010
Accepted 22 December 2010

Keywords:
MSCT
ARDS
ECMO
H1N1
Swine-origin influenza A infection

ABSTRACT

Purpose: The purpose of this study was to retrospectively evaluate whether computed tomography (CT) findings have prognostic value for the prediction of mortality and severity of the clinical course in patients presenting with early stage of acute respiratory distress syndrome (ARDS) due to swine-origin influenza A (S-OIV).
Materials and methods: Chest CT (16-/64-row multidetector CT) of 23 patients (of whom 9 patients died) were retrospectively reviewed by three independent blinded observers. The CT findings were graded on a 3-point scale (1: normal attenuation, 2: ground-glass attenuation, 3: consolidation). The extent of each abnormality was determined by visually estimating the percentage (to the nearest 10%) of the affected lung parenchyma in each zone and multiplied by the CT-score described above.
Results: All patients presented with a mixture of bilateral patchy consolidations and ground glass opacities. Spearman rank correlation in evaluation of the presence and extent of lung abnormalities by the three different observers was good (correlation coefficient, 0.876–0.922; $p < 0.001$). The overall CT-score in survivors (mean, 96.0 (±26.2); range, 53–158) was significantly lower than that in non-survivors (mean, 116.2 (±14.0); range, 101–139). ROC analysis revealed an area under curve of 0.79 ($p = 0.021$) for the CT score with an optimal cutoff value of a CT-score of 100 for prediction of survival, with a sensitivity of 100% and a specificity of 64% (accuracy, 78%). For this optimal cutoff, Kaplan–Meier estimator showed a significant difference for the survival ratio ($p = 0.011$).
Conclusion: In patients with severe ARDS due to S-OIV-infection, the CT-score has a prognostic value in the prediction of mortality.

1. Introduction

Swine-origin influenza A (S-OIV; H1N1 2009) had been described initially in Mexico in April 2009 and has spread rapidly all over the world since then [1]. In June 2009, the World Health Organization (WHO) raised the alert level to pandemic phase 6 for the S-OIV infection [2]. Until August 2010, worldwide more than 214 countries have reported laboratory confirmed cases of pandemic influenza H1N1 2009, including over 18,449 deaths [3]. In most cases, mild clinical symptoms with influenza-like illness is present, however, acute respiratory distress syndrome (ARDS) may occur in some cases. ARDS is a severe clinical condition that requires a multimodal treatment approach [4,5]. This includes in severe cases invasive adjuvant strategies, for instance extracorporal membrane oxygenation (ECMO), that may reduce the ventilator-induced lung injury and mortality [6,7]. Mortality varies due to inhomogeneous patient collective. According to the published data approximately 35–60% of patients with ARDS die in the course of the disease [8].

The general radiological findings in ARDS are ground-glass opacity and airspace consolidation mostly in the basal and posterior parts. Viral pneumonias in general are represented by poorly defined nodules, patchy areas of peribronchal ground-glass opacity, and air-space consolidation; hyperinflation is commonly present due to the associated bronchiolitis [9]. The progressive form of viral pneumonia shows rapidly confluent areas of diffuse alveolar damage, consisting of homogeneous or patchy unilateral or bilateral air-space consolidation and ground-glass opacity or poorly defined centrilobular nodules [10]. Recent studies of S-OIV infection in adults have reported radiographic findings in patients with an advanced clinical course of S-OIV infection and radiologic patterns in the pediatric patient population [9,11–14]. Chest CT patterns and

* Corresponding author at: Klinik für Strahlenheilkunde, Charité–Universitätsmedizin Berlin, Campus Virchow-Klinikum, Augustenburger Platz 1, 13353 Berlin, Germany. Tel.: +49 30 450657483; fax: +49 30 450557901.
E-mail address: christian.grieser@charite.de (C. Grieser).
[1] Shared first authorship.

0720-048X/$ – see front matter © 2011 Elsevier Ireland Ltd. All rights reserved.
doi:10.1016/j.ejrad.2010.12.085

their eventual prognostic value in ARDS, however, remain to be investigated.

The aim of the present study was to retrospectively evaluate whether the CT appearance can predict mortality in patients with a clinically early stage of ARDS in patients with microbiologically confirmed S-OIV infection.

2. Materials and methods

2.1. Patients

A total of 23 consecutive patients suffering from ARDS (female, 7; male, 16; mean age, 42.2 ± 16 years), who had chest CT upon clinical onset of laboratory confirmed H1N1 related ARDS, were transferred to our center of specialty between November 2009 and February 2010 for further intensive care and ECMO therapy if necessary. A complete digital CT-dataset of the lung and a comprehensive clinical documentation had to be present. The retrospective study was approved by the institutional review board.

2.2. Computed tomography

CT data were obtained with 16- or 64-row (Lightspeed Pro16, Lightspeed VCT; GE Medical Systems, Milwaukee, IL) multidetector CT. After injection of iodinated non-ionic contrast material (iopromide [Ultravist 370®; BayerSchering Pharma, Berlin, Germany]; volume, 100 mL; flow, 2.5 mL/s) a contrast-enhanced examination of the entire thorax and abdomen during venous phase (60 s delay) was acquired (voltage, 120 kV; tube current (regulated by automatic dose modulation), 100–350 mA; rotation time, 0.7 s; detector collimation, 16 mm × 1.25 mm and 64 mm × 0.625 mm; table feed, 35 mm/gantry rotation). Primary image reconstruction was performed at a slice thickness of 1.25 mm (increment, 0.5) using a lung kernel.

2.3. Image analysis

For CT analysis, a dedicated viewing workstation (Advantage Windows 4.3; GE Medical Systems) was used. Three experienced radiologists (2, 5, and 22 years of experience in thoracic CT reading) independently evaluated all CT data. The reviewers were aware of the diagnosis of S-OIV infection, but they were blinded to clinical data.

The CT findings were graded on a 3-point scale on the basis of the classification system previously described [15,16], score of 1, normal attenuation; score of 2, ground-glass attenuation; score of 3, consolidation. Ground-glass opacity was diagnosed when there was a hazy area of increased opacity without obscuration of the underlying vessels and airway walls. Consolidation was defined as an area of increased opacity that obscured the margins of vessels and airway walls, with or without air bronchograms.

The presence of the abnormalities described above was assessed independently in three (upper, middle, and lower) zones of each lung (in total 6 zones). The upper zone was defined as the area above the level of the carina, the middle zone as the area between the level of the carina and the level of infrapulmonary vein, and the lower zone as the area below the level of infrapulmonary vein. The extent of each abnormality was determined by visually estimating the percentage (to the nearest 10%) of the affected lung parenchyma in each zone and multiplied by the classification system described above. The assessments of the three observers were averaged. The overall CT score for each patient was obtained by adding the six averaged scores. Furthermore, the Hounsfield Units (HU) of the different zones were measured. The pleural space was evaluated for the presence of effusion; heart effusion was also evaluated. The hila and the mediastinum were evaluated for lymphadenopathy.

2.4. Clinical data

Age, sex, underlying medical conditions, clinical scores and clinical outcome from S-OIV infection were recorded for each patient. Severity of illness was assessed using the Simplified Acute Physiology Score (SAPS II) score [17], the Sequential Organ Failure Assessment (SOFA) score [18], the Acute Physiology and Chronic Health Evaluation (APACHE II) score [19], and the Murray Lung Injury score [20]. The Lung Injury score describes the severity of lung failure based on four entities: PEEP, compliance, number of consolidation quadrants on chest x-ray and P/F ratio. Mortality is not predicted by the Murray score [6]. Endpoints of the study were death or transfer from intensive care unit.

2.5. Statistical analysis

Statistical analyses were performed using the SPSS-software (release 11.0.4; SPSS Inc., Chicago, IL) and the R software (Version 2.8.1; The R Foundation for Statistical Computing, Vienna, Austria). Data are expressed as mean (± standard deviation (SD)). Interobserver variability was assessed with spearman rank correlation coefficient. Differences between survivors and non-survivors and ECMO and non-ECMO patients were analyzed by using the Mann–Whitney *U*-test. Receiver operator characteristic (ROC) curves were used to analyse the association of the CT-score. The optimal cut-off value was defined by the point on the ROC curve with the minimal distance between the 0% false positive and the 100% true positive rate. To estimate the survival ratio Kaplan–Meier estimator was used. For all statistical analyses a *p*-value of less than 0.05 was considered to indicate a significant difference.

3. Results

3.1. Baseline clinical characteristics

The CT Data of 23 (male, 16; female, 7, of which 3 were pregnant) patients, of whom 9 patients died, were retrospectively analyzed. A subset of patients ($n = 12$) received ECMO therapy with 50% survival. Two patients presented with chronic lung diseases: one had lung metastases from germinoma, the other patient had lung fibrosis (this information was provided to the reviewers to enable differentiation of the nodules and the fibrotic changes from the ARDS-related findings). Two patients had a chronic lymphatic leukemia. One patient was HIV-positive, and 1 patient had a common variable immunodeficiency. The demographic data and clinical parameters on the day of CT for all 23 patients are shown in Tables 1 and 2. Regarding the age, a significant difference for survivors and non-survivors was found ($p = 0.016$); for the sex no significant difference was found ($p > 0.05$), Table 1.

3.2. CT findings and score

All patients presented with a mixture of patchy consolidations and ground glass opacities (Fig. 1). The abnormalities were bilateral in all of the 23 patients; nodular opacities (except the metastatic lesions in 1 patient) were not evident on CT. The distribution of parenchymal abnormalities was diffuse without regional predominance in 17 patients (74%). In 6 patients, the changes were seen predominantly in the lower lung fields (24%). Sixteen patients presented with pleural effusions (70%); none of the patients had a heart effusion; 2 patients had hilar and mediastinal lymphadenopathy (9%). Spearman rank correlation in evaluation of the presence

Table 1
Clinical characteristics of patients with ARDS at time of CT Examination (survivors versus non-survivors).

Characteristics	All patients	Survivors	Non-survivors	p-Value
Number	23	14	9	
Age	42.2 ± 16.4	36.2 ± 15.1	51.5 ± 14.5	$p = 0.016$
Sex				
Male	16	10	6	NS
Female	7	4	3	NS
Time from onset (days)	3.55 ± 2.1	3.71 ± 3	3.46 ± 1.5	NS
Chronic lung disease	3	0	3	NS
Pregnancy	3	3	0	NS
HIV	1	1	0	NS
Common variable immunodeficiency	1	0	1	NS
Chronic lymphatic leukemia	2	0	2	NS
CT score	103.9 ± 24.0	96.0 ± 26.2	116.2 ± 14.0	$p = 0.021$
Distribution of findings				
Diffuse	17	10	7	NS
Dorsal	6	4	2	NS
SAPS II	54.7 ± 17.3	48.9 ± 17.6	63.1 ± 13.7	$p = 0.038$
SOFA	12.4 ± 3.1	12.1 ± 3.2	12.9 ± 3.2	NS
APACHE II	26.8 ± 10.3	22.1 ± 9.5	33.6 ± 7.4	$p = 0.008$
Murray	3.4 ± 0.4	3.3 ± 0.4	3.7 ± 0.4	$p = 0.003$
P/F ratio (p_aO_2/FiO_2)	91.3 ± 45.2	101.5 ± 53.4	75.6 ± 23.0	NS
P/F score (oxygenation index)	3.6 ± 0.7	3.4 ± 0.8	3.9 ± 0.4	NS

Table 2
Clinical characteristics of patients with ARDS and following ECMO therapy at time of CT examination.

Characteristics	All patients	ECMO therapy	Non-ECMO therapy	*p*-Value
Number	23	12	11	NS
Survivors	14	6	8	NS
Age	42.2 ± 16.38	42.66 ± 15.98	41.69 ± 17.58	NS
Sex				
Male	16	7	9	NS
Female	7	5	2	NS
Time from onset (days)	3.55 ± 2.1	3.71 ± 3	3.46 ± 1.5	NS
Chronic lung disease	3	3	0	NS
Pregnancy	3	2	1	NS
HIV	1	1	0	NS
Common variable immunodeficiency	1	1	0	NS
Chronic lymphatic leukemia	2	2	0	NS
CT score	103.91 ± 24.04	115 ± 19.56	91.82 ± 23.29	$p = 0.022$
Distribution of findings				
Diffuse	17	8	9	NS
Dorsal	6	4	2	NS
SAPS II	54.73 ± 17.32	54.83 ± 17.17	55.8 ± 18.36	NS
SOFA	12.41 ± 3.13	13.83 ± 3.33	10.7 ± 1.83	$p = 0.013$
APACHE II	26.77 ± 10.3	27.25 ± 10.83	26.2 ± 10.16	NS
Murray	3.43 ± 0.42	3.69 ± 0.26	3.13 ± 0.38	$p = 0.002$
P/F ratio (p_aO_2/FiO_2)	91.34 ± 45.22	66.83 ± 20.99	118.08 ± 50.07	$p = 0.004$
P/F score (oxygenation index)	3.59 ± 0.67	3.83 ± 0.39	3.3 ± 0.82	$p = 0.077$

of these abnormalities by the three different observers was high (correlation coefficient, 0.876–0.922; $p < 0.001$).

The overall CT score in survivors (mean, 96 (±26.2); range, 53–158) was significantly lower than that in non-survivors (mean, 116.2 (±14.0); range, 101–139; Table 1; Fig. 2). ROC analysis revealed an area under the curve (AUC) of 0.79 ($p = 0.021$) for the CT score with an optimal cutoff value of a CT score of 100 for prediction of survival (sensitivity, 100%; specificity, 64%; accuracy, 78%; Fig. 3). For this optimal cutoff, Kaplan–Meier estimator showed a significant difference for the survival ratio ($p = 0.011$; Fig. 4).

The overall CT score in patients with ECMO therapy (mean, 115 (±19.6); range, 89–158) was significantly higher than the score

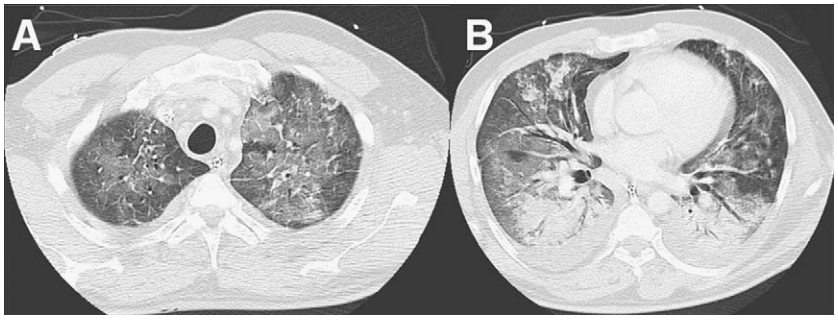

Fig. 1. CT of a 47 year old male patient (no survival; CT score of 117) with ground glass opacity mostly in the upper parts (A) and consolidation in the lower parts (B).

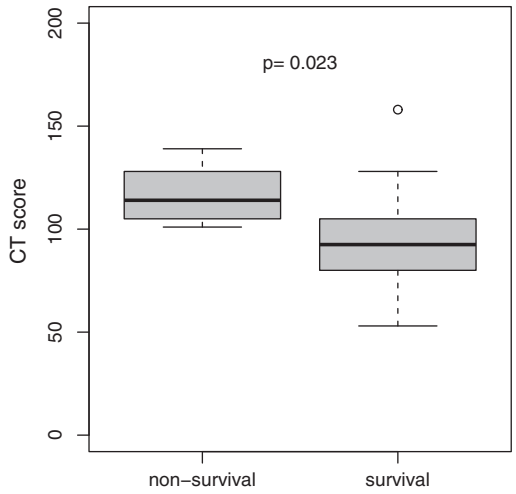

Fig. 2. CT score for prediction of survival.

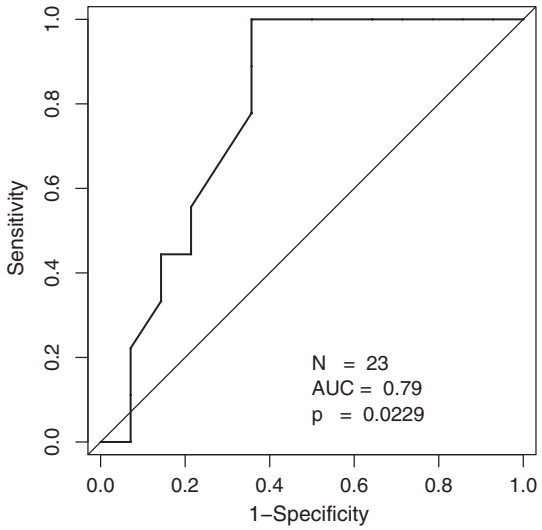

Fig. 3. ROC analysis of the CT score for prediction of survival.

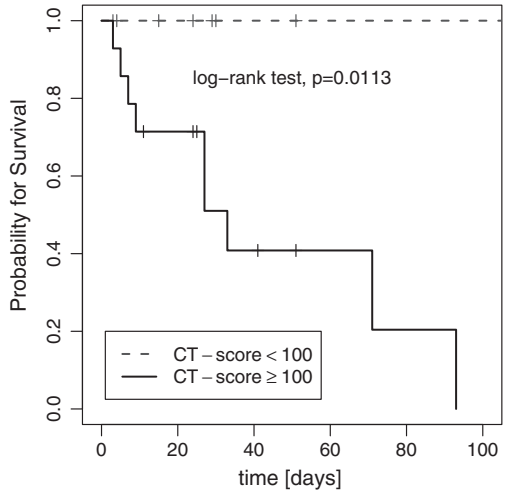

Fig. 4. Kaplan–Meier estimator showed a significant difference for the survival ratio for a CT-Score cut-off of 100.

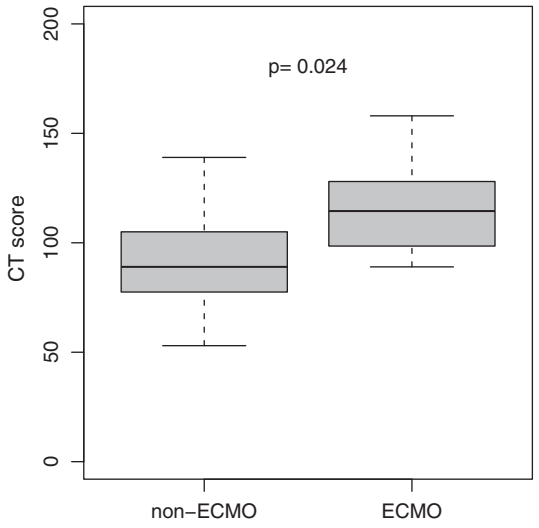

Fig. 5. CT score of patients with ECMO therapy.

in patients without ECMO therapy (mean, 91.8 (±23.3); range, 53–139; Table 2; Fig. 5). ROC analysis revealed an AUC of 0.78 ($p = 0.022$) for the CT score with an optimal cutoff value of a CT score of 98.5 for prediction of ECMO therapy (sensitivity, 75%; specificity, 54%; Fig. 6).

The results for the clinical scores on the day of CT are shown in Tables 1 and 2. Regarding mortality, a significant difference for survival was found for the APACHE II ($p = 0.008$), SAPS II ($p = 0.038$) and the Murray ($p = 0.003$) score (Table 1). The SOFA score was not significant in our patient collective ($p > 0.05$). However, only for the Murray score, a significant correlation to the CT score was found (Spearman rank correlation coefficient, 0.59; $p = 0.003$) whereas correlation for the CT score and all other clinical scores were not significant ($p > 0.05$). The SOFA ($p = 0.013$) and Murray ($p = 0.002$) scores were significantly higher in the ECMO group whereas the APACHE II and SAPS II scores were not significantly different ($p > 0.05$, Table 2).

For areas with normal attenuation, the averaged score was −698.5 (±124.1) HU, for ground-glass attenuation −326.7 (±149.3) HU, and for consolidation 9.6 (±68.3) HU.

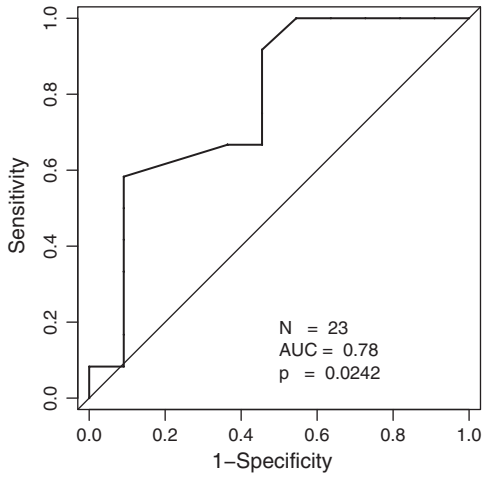

Fig. 6. ROC analysis of the CT score for prediction of ECMO therapy.

4. Discussion

ARDS is an inflammatory disorder of the lung, which is acute in onset and characterized by arterial hypoxemia due to increased intrapulmonary shunt perfusion and diffuse radiological infiltrates in the absence of clinical evidence of left atrial hypertension [21]. ARDS can be caused by a variety of insults including viral pneumonias such as S-OIV infection. Most cases with S-OIV infection are mild and self-limited, but a small percentage of patients have a severe course that may result in ARDS [22]. The high-risk group includes young children and older adults; this is reflected by the fact that we found a significant difference for the age in survivors and non-survivors. Furthermore, analogue to our results, patients with chronic underlying conditions and immunosuppressed patients have a higher risk for an increased mortality. A high APACHE II ($p = 0.008$), SAPS II ($p = 0.038$) and Murray ($p = 0.003$) score are independently associated with mortality, which is reflected by our results. For the Murray score, this is in contrast to previous results as described by Rubenfeld and Herridge [8]. However, only for the Murray score, a significant correlation to the CT score was found ($p = 0.003$; correlation coefficient of 0.59). This is not surprising as the Murray score is the clinical score which reflects pulmonary function and where the numbers of quadrants with infiltration seen on chest x-ray are included [20]. All other clinical scores include different clinical parameters [17–19]. The SOFA score, which is also known as an important predictor of survival, was not significant in our patient collective ($p > 0.05$; [15,23,24]. However, this may be due to the high baseline SOFA score in our patient population (range, 10–12) which means that most of the patients already had a three or four organ failure (lung, circulation, kidney, coagulation) and CNS or liver failure is rarely seen in our patient collective.

Other studies described nodular opacities in viral pneumonias [25]. However, previous reports of influenza have shown patchy areas of ground-glass attenuation mixed with consolidation [9,22,26–28]. All our patients with a severe ARDS due to S-OIV infection presented with a mixture of patchy consolidations and ground glass opacity. Marchiori et al. stated, that patients who exhibit consolidations on CT have a more severe clinical course than those who present with ground-glass opacities, furthermore, these abnormalities can be pathologically correlated with diffuse alveolar damage [12]. In our study, average HU score was −326.7 (±149.3) for ground-glass attenuation and 9.64 (±68.3) for consolidation areas. None of the patients had nodular opacities or reticular pattern such as architectural distortion and traction bronchiectasis or bronchiolectasis and honeycombing (except the patient with known pre-existing lung fibrosis). Ichikado and colleagues observed that certain CT findings correlate with the stages of diffuse alveolar damage [15,16] Therefore, architectural distortion and traction bronchiectasis or bronchiolectasis were almost invariably associated with the late proliferative or fibrotic phases of ARDS. The distribution of parenchymal abnormality was diffuse without regional predominance in most patients ($p > 0.001$). Follow-up studies after treated ARDS have revealed that many patients have residual morphologic lung injury such as chronic pulmonary fibrosis [29–31]. High-pressure ventilation may lead to hyperinflation of non-atelectatic lung segments causing a ventilator induced lung injury (VILI) predominantly in the ventral lung sections [30]. However, in our study, no follow up CT data was available for all of the patients. Therefore, further studies are necessary to prove this statement for S-OIV related ARDS.

All our patients required mechanical ventilation; 9 patients died. The overall CT score was significantly lower in survivors compared to non-survivors ($p = 0.021$). Regarding the prediction of survival, we found an optimal cutoff value of a CT score of 100 (accuracy of 78%). For this optimal cutoff, a significant difference for the survival ratio was found ($p = 0.011$). A subset of our patients ($n = 12$) underwent therapy intensification due to their poor clinical and respiratory condition with ECMO therapy; 6 of whom died. In patients treated with ECMO chronic underlying conditions, immunosuppression, and pregnancy were more frequently present. The SOFA ($p = 0.013$) and Murray ($p = 0.002$) scores were significantly higher in the ECMO group whereas the APACHE II and SAPS II scores were not significantly different ($p > 0.05$). The overall CT score in patients with ECMO therapy was significantly higher than that in patients without ECMO therapy ($p = 0.022$). The optimal cutoff value of the CT score for prediction of an ECMO therapy was 98.5 with a sensitivity of 75% and a specificity of 54%. However, these patients treated with ECMO therapy presented with a severe disease and may not have survived without this therapy treatment.

Spearman rank correlation in evaluation of the presence of lung abnormalities by the three different observers was good (correlation coefficient, 0.876–0.922; $p < 0.001$).

All our CT examinations were performed in expiratory breath-hold. However, Helm et al. stated that inspiratory breath-hold CT will overestimate the degree of lung aeration and underestimate the degree of atelectasis; conversely expiratory breath-hold CT is likely to underestimate aerated lung and overestimate atelectatic lung [32]. Therefore, dynamic CT is potentially more accurate than traditional breath-hold CT in the assessment of ARDS; however, in terms of clinical application, radiation dose might be a limiting factor for the use of dynamic CT [32].

Regarding possible limitations of the study, the small sample size has to be mentioned. Furthermore, preexisting diseases of the lung, like present in two of the patients, can bias the CT score. However, S-OIV infection will also occur in chronic pulmonary disease and it is a common quest for radiologists to tell chronic and acute changes apart even without prior examinations available, which was possible in the present two cases. Concerning the intensified therapy using ECMO therapy, results might be hampered by the therapy decision, which is of course an individual decision influenced by many factors, even though a standardized decision algorithm exists. Whether this explains the limited (but still significantly accurate) ability of the CT score to foresee the necessity of ECMO despite good correlation with a variety of clinical scoring systems, or whether the mortality prediction was falsified by successful salvage therapy using ECMO cannot be concluded from the present data.

In conclusion, we have evaluated the prognostic implication of a CT score assessed by determining the extent of patchy areas of ground-glass attenuation mixed with consolidation at imaging in patients in the early stage of ARDS from S-OIV infection. With this CT score, risk stratification can be done. Furthermore, in combination with the presented clinical scores and the therapy outcome, the CT score may play a role in therapy decision making in the future, especially regarding intensified therapy with ECMO.

Conflict of interest

All author have no financial relationship to disclosure.

References

[1] Perez-Padilla R, de la Rosa-Zamboni D, Ponce de Leon S, et al. Pneumonia and respiratory failure from swine-origin influenza A (H1N1) in Mexico. N Engl J Med 2009;361(13):680–9.
[2] Global alert and response: pandemic (H1N1) 2009: update 64. World Health Organization Web site.
[3] Global alert and response: pandemic (H1N1) 2009: update 112. World Health Organization Web site.
[4] Abraham E, Matthay MA, Dinarello CA, et al. Consensus conference definitions for sepsis, septic shock, acute lung injury, and acute respiratory distress syndrome: time for a re-evaluation. Crit Care Med 2000;28:232–5.
[5] Lewandowski K, Lewandowski M. Epidemiology of ARDS. Minerva Anestesiol 2006;72:473–7.

[6] Deja M, Hommel M, Weber-Carstens S, et al. Evidence-based therapy of severe acute respiratory distress syndrome: an algorithm-guided approach. J Int Med Res 2008;36:211–21.
[7] Bartlett RH, Roloff DW, Custer JR, et al. Extracorporeal life support: the University of Michigan experience. JAMA 2000;283(16):904–8.
[8] Rubenfeld GD, Herridge MS. Epidemiology and outcomes of acute lung injury. Chest 2007;131:554–62.
[9] Marchiori E, Zanetti G, Hochhegger B, et al. High-resolution computed tomography findings from adult patients with Influenza A (H1N1) virus-associated pneumonia. Eur J Radiol 2010;74:93–8.
[10] Kim EA, Lee KS, Primack SL, et al. Viral pneumonias in adults: radiologic and pathologic findings. Radiographics 2002;22:S137–49.
[11] Li P, Su DJ, Zhang JF, Xia XD, Sui H, Zhao DH. Pneumonia in novel swine-origin influenza A (H1N1) virus infection: high-resolution CT findings. Eur J Radiol. 2010 Jun 19. [Epub ahead of print].
[12] Marchiori E, Gláucia Zanetti G, Asvolinsque Pantaleão Fontes C, et al. Influenza A (H1N1) virus-associated pneumonia: high-resolution computed tomography–pathologic correlation. Eur J Radiol. 2010 Oct 28. [Epub ahead of print].
[13] Zhao C, Gan Y, Sun J. Radiographic study of severe Influenza-A (H1N1) disease in children. Eur J Radiol. 2010 Oct 19. [Epub ahead of print].
[14] Ketelsen D, Haap M, Overkamp D, et al. Imaging of pulmonary complications of novel influenza A infection (H1N1). Rofo 2010;182:103–5.
[15] Ichikado K, Suga M, Muranaka H, et al. Prediction of prognosis for acute respiratory distress syndrome with thin-section CT: validation in 44 cases. Radiology 2006;238:321–9.
[16] Ichikado K, Suga M, Muller NL, et al. Acute interstitial pneumonia: comparison of high-resolution computed tomography findings between survivors and nonsurvivors. Am J Respir Crit Care Med 2002;165(1): 1551–6.
[17] Le Gall JR, Lemeshow S, Saulnier F. A new Simplified Acute Physiology Score (SAPS II) based on a European/North American multicenter study. JAMA 1993;270:(22–29):2957–63.
[18] Vincent JL, Moreno R, Takala J, et al. The SOFA (sepsis-related organ failure assessment) score to describe organ dysfunction/failure. On behalf of the working group on sepsis-related problems of the European Society of Intensive Care Medicine. Intens Care Med 1996;22:707–10.
[19] Knaus WA, Draper EA, Wagner DP. APACHE.I.I.a severity of disease classification system. Crit Care Med 1985;13:818–29.
[20] Murray JF, Matthay MA, Luce JM, et al. An expanded definition of the adult respiratory distress syndrome. Am Rev Respir Dis 1988;138:720–3.
[21] Bernard GR, Artigas A, Brigham KL, et al. Report of the American-European Consensus conference on acute respiratory distress syndrome: definitions, mechanisms, relevant outcomes, and clinical trial coordination. Consensus committee. J Crit Care 1994;9:72–81.
[22] Ajlan AM, Quiney B, Nicolaou S, et al. Swine-origin influenza A (H1N1) viral infection: radiographic and CT findings. Am J Roentgenol 2009;193:1494–9.
[23] Monchi M, Bellenfant F, Cariou A, et al. Early predictive factors of survival in the acute respiratory distress syndrome. A multivariate analysis. Am J Respir Crit Care Med 1998;158:1076–81.
[24] Estenssoro E, Dubin A, Laffaire E, et al. Incidence, clinical course, and outcome in 217 patients with acute respiratory distress syndrome. Crit Care Med 2002;30:2450–6.
[25] Reittner P, Ward S, Heyneman L, et al. Pneumonia: high-resolution CT findings in 114 patients. Eur Radiol 2003;13:515–21.
[26] Mollura DJ, Asnis DS, Crupi RS, et al. Imaging findings in a fatal case of pandemic swine-origin influenza A (H1N1). Am J Roentgenol 2009;193:1500–3.
[27] Agarwal PP, Cinti S, Kazerooni EA. Chest radiographic and CT findings in novel swine-origin influenza A (H1N1) virus (S-OIV) infection. Am J Roentgenol 2009;193:1488–93.
[28] Aviram G, Bar-Shai A, Sosna J, et al. H1N1 influenza: initial chest radiographic findings in helping predict patient outcome. Radiology 2010;255:252–9.
[29] Linden VB, Lidegran MK, Frisen G, et al. ECMO in ARDS: a long-term follow-up study regarding pulmonary morphology and function and health-related quality of life. Acta Anaesthesiol Scand 2009;53:489–95.
[30] Nobauer-Huhmann IM, Eibenberger K, Schaefer-Prokop C, et al. Changes in lung parenchyma after acute respiratory distress syndrome (ARDS): assessment with high-resolution computed tomography. Eur Radiol 2001;11:2436–43.
[31] Desai SR, Wells AU, Rubens MB, et al. Acute respiratory distress syndrome: CT abnormalities at long-term follow-up. Radiology 1999;210:29–35.
[32] Helm E, Talakoub O, Grasso F, et al. Use of dynamic CT in acute respiratory distress syndrome (ARDS) with comparison of positive and negative pressure ventilation. Eur Radiol 2009;19:50–7.